

Shortest Path Lengths in Poisson Line Cox Processes: Approximations and Applications

Gourab Ghatak *Member, IEEE*, Sanjoy Kumar Jhawar, and Martin Haenggi, *Fellow, IEEE*

Abstract—We derive exact expressions for the shortest path length to a point of a Poisson line Cox process (PLCP) from the typical point of the PLCP and from the typical intersection of the underlying Poisson line process (PLP), restricted to a single turn. For the two turns case, we derive a bound on the shortest path length from the typical point and demonstrate conditions under which the bound is tight. We also highlight the line process and point process densities for which the shortest path from the typical intersection under the one turn restriction may be shorter than the shortest path from the typical point under the two turns restriction. Finally, we discuss two applications where our results can be employed for a statistical characterization of system performance: in a re-configurable intelligent surface (RIS) enabled vehicle-to-vehicle (V2V) communication system and in electric vehicle charging point deployment planning in urban streets.

Index Terms—Line process, point process, Cox process, V2V communications, path lengths, stochastic geometry.

I. INTRODUCTION

Line or hyperplane processes are critical statistical models used to address various engineering issues in transportation and urban infrastructure planning, wireless communications, and industrial automation [1], [2]. In the Euclidean plane, these processes represent the set of points that constitute lines on the plane, where the locations and orientations of the lines are specified on a parameter space according to a spatial point process. In particular, the Poisson line process (PLP) is a stochastic model used to describe random patterns of lines on a plane, where the lines are generated by a Poisson point process (PPP) in the parameter space. Researchers utilize line processes to investigate doubly stochastic processes called Cox processes, which are Poisson point processes constrained on the line process as their domain [3]–[7]. These models are instrumental in solving engineering questions, such as planning for the number of electric vehicle charging stations and bus stops, analyzing the cellular coverage performance for urban users with on-street deployments of wireless small cells [8], etc.

The ℓ_1 distance is a metric that measures the shortest path between two points when the movement is restricted to the lines of the PLP. This is particularly important for transportation networks since it characterizes the distance traveled by a vehicle or pedestrian along the streets. Despite the relevance of this metric for practical applications, the characteristics and computational methods for ℓ_1 distances in the Poisson line Cox process (PLCP) are not well understood. Fig. 1 illustrates the

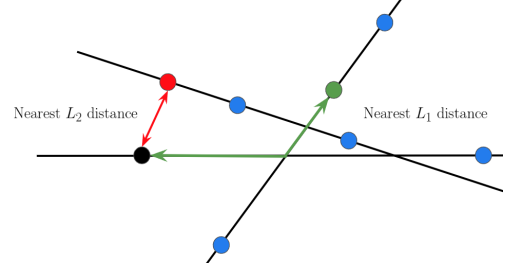


Fig. 1. Illustration of the nearest ℓ_2 vs ℓ_1 distances. From the perspective of the typical point (black), the red point is the nearest point of the PLCP in the Euclidean plane, while, the green point is the nearest point from a path length perspective.

difference between the nearest neighbor with respect to the Euclidean distance in contrast to the same in terms of the path length. Although the nearest ℓ_2 distance is simple to derive, e.g., see [8], [9], the same is not true for the shortest path-length or the ℓ_1 distance.

Researchers have studied the shortest path length distributions for the case of the Manhattan line Cox process [10], where the orientations of the lines are restricted to a discrete set of two angles $\{0, \pi/2\}$. This was further extended to study dynamic charging of electric vehicles in [11]. For the PLCP model, the authors of [12] have proposed a method for simple computation of the mean shortest path lengths leveraging Neveu’s exchange formula [13]. The asymptotic behavior of this shortest path distance is investigated in [14]. However, due to the random orientation of the lines in a PLP, the exact characterization of the distribution of the shortest path length is challenging, and is still an open problem.

Contributions: Restricted to the one turn case (to be shortly defined), we provide an exact characterization of the shortest path length distribution to a point of the PLCP from the typical point of a PLCP and from the typical intersection of the underlying PLP. The case for the typical intersection is technically challenging and needs careful consideration of locations that are within a given path-length along both the lines constituting the typical intersection. Furthermore, we derive a bound on the shortest path length distribution for the two-turns case from the typical point of the PLCP. We study the conditions in which the path may be shorter for the one-turn case from the typical intersection as compared to the two-turn case starting from the typical point. Our results will find applications both in wireless network analysis, especially in vehicular communications, as well as planning of street systems. We discuss two such applications, one on optical vehicle-to-vehicle (V2V) communications that leverage re-configurable intelligent surface (RIS) and the other on planning for the placement of electric vehicle charging points.

G. Ghatak is with Department of Electrical Engineering, IIT Delhi, Hauz Khas, India 110016. Email: gghatak@ee.iitd.ac.in. S. K. Jhawar is with the DYOGENE team, INRIA Paris, France. Email: sanjoy-kumar.jhawar@inria.fr. M. Haenggi is with the Department of Electrical Engineering, University of Notre Dame, Notre Dame, IN 46556 USA (e-mail: mhaenggi@nd.edu).

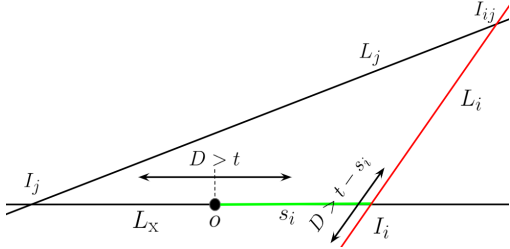


Fig. 2. Approximation using recursive equations

II. BACKGROUND AND NOTATION

A line process in \mathbb{R}^2 is a set of points in \mathbb{R}^2 that constitute a set of lines. Each line L_i is uniquely characterized by its signed distance r_i from the origin and the angle θ_i that the normal to the line makes with the x -axis. The parameter pair (θ_i, r_i) thus resides as a point in a parameter space $[0, \pi) \times (-\infty, \infty)$ that generates the line L_i in \mathbb{R}^2 .

Definition 1. A line process $\mathcal{P} \subset \mathbb{R}^2$ is called a PLP iff the generating points form a PPP on the parameter space $[0, \pi) \times (-\infty, \infty)$ with a constant density λ .

Then, the points of the PLP that comprise $L_i \subset \mathcal{P}$ is the set $\{(x, y) \in \mathbb{R}^2 : x \cos \theta_i + y \sin \theta_i = r_i \text{ for some } (\theta_i, r_i) \in [0, \pi) \times (-\infty, \infty)\}$. Let us consider one such PLP \mathcal{P} where the intensity of the generating points is λ . On each $L_i \subset \mathcal{P}$, let us define a one dimensional PPP $\Phi_i \subset L_i$ with intensity μ . The collection of all such one dimensional PPPs on all such lines $\Phi := \cup_{i: L_i \subset \mathcal{P}} \Phi_i$ is called a PLCP with intensity parameters λ and μ . Furthermore, we denote by I_{ij} as the point of intersection of L_i and L_j , and define the intersection process as $\Phi_I := \cup_{i,j: L_i, L_j \subset \mathcal{P}} I_{ij} = \cup_{i,j \in \mathcal{P}} L_i \cap L_j$. We perform our analysis from the perspective of the typical point of Φ . In particular, let us define

$$\Phi^o \triangleq (\Phi \mid o \in \Phi),$$

and note that under expectation over Φ^o , o becomes the typical point of the process Φ . Since by construction, Φ is a stationary process, let us consider o to be the origin of \mathbb{R}^2 . Under Palm conditioning, there exists a line L_x passing through o . Without loss of generality, let us consider L_x to be the x -axis. Let the lines intersecting L_x be enumerated (in no particular order) by the elements of the set $\{L_i\}$, $i \in \mathbb{N}$ and the corresponding intersections be $\{I_i\}$. Let the distance of I_i from the origin be denoted by s_i and the angle between L_1 and L_x be denoted by θ_i . Let D denote the length of the shortest path from the typical point to the nearest neighbor of the PLCP. Mathematically,

$$D = \min_{x \in \Phi^{!o}} \|x\|_1,$$

where $\Phi^{!o}$ is the reduced Palm process constructed by assuming the typical point to be a part of Φ and then by removing the typical point.

A. Limitation of a trivial approximation

Note that a simple approximation as illustrated in Fig. 2 follows by assuming that the distribution of the shortest path length from the typical PLCP point is the same as the

distribution of the shortest path length from I_i conditioned on the event that the path from I_i cannot start along L_x but along L_i . In Fig. 2 it means that at I_i , we remove the line L_x and consider I_i as the surrogate of the typical point and study the event $D > t - s_i$. Mathematically, this results in the following recursive equation.

$$\mathbb{P}(D > t) = \exp(-\mu t) \sum_k p_k(t) \left(\frac{1}{t} \int_0^t \mathbb{P}(D > t - s) ds \right)^k,$$

where $p_k(t) := \exp(-2\lambda t) \frac{(2\lambda t)^k}{k!}$, is the probability that there are k intersections within a distance t from the typical point. Conditioned on k , the distances of these intersections are independent and identically (in fact uniformly) distributed in $[0, t]$. As per the approximation, given that an intersection is at a distance s from the typical point on L_x , for no points within a path length t from the typical point, we are interested in the event $D > t - s$ from the intersection. Thus, we get

$$\mathbb{P}(D > t) = \exp(-\mu + 2\lambda)t \sum_k \frac{1}{k!} \left(2\lambda \int_0^t \mathbb{P}(D > t - s) ds \right)^k,$$

Now defining $u(t) := \mathbb{P}(D > t)$, $I(t) := \int_0^t u(t - s) ds$ and differentiating with respect to t we obtain the following differential equation.

$$\begin{aligned} u'(t) &= \exp(-(\mu + 2\lambda)t) \sum_k \frac{1}{(k-1)!} \left(2\lambda \int_0^t u(t-s) ds \right)^{k-1} \\ &\frac{d}{dt} \left(2\lambda \int_0^t u(t-s) ds \right) - (\mu + 2\lambda)u(t) \\ &= \exp(-(\mu + 2\lambda)t) 2\lambda \sum_k \frac{1}{(k-1)!} \\ &\left(2\lambda \int_0^t u(t-s) ds \right)^{k-1} - (\mu + 2\lambda)u(t) \\ &= 2\lambda u(t) - (\mu + 2\lambda)u(t) = -\mu u(t). \end{aligned}$$

This solution results in

$$\mathbb{P}(D > t) = \exp(-\mu t),$$

which is incidentally the same as the probability of no PLCP point being located within a distance t on L_x from the typical point. This occurs due to the fact that while approximating the path length from I_i to be D , we over-count segments of the PLP, e.g., the segment between the typical point and I_i shown in green in Fig. 2. This motivates the need for a more careful characterization of the path length distribution.

III. SINGLE TURN CASE

Let us first consider the distribution of the distance to the nearest neighbor from the typical point under the restriction that only those PLCP points are considered that are reachable by traversing at most two lines L_i , including L_x . Within this restriction, we consider two cases: first where the origin is the typical point and second where the origin is the typical intersection.

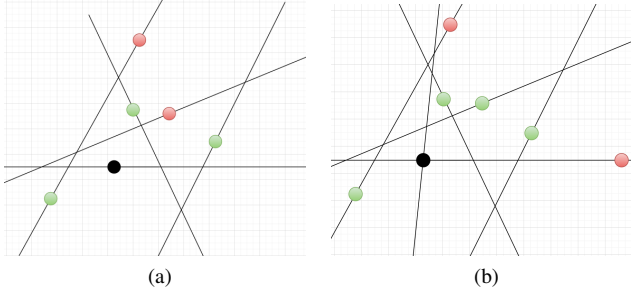


Fig. 3. All the green colored points are within a distance t by taking at most one turn from the origin (black point) when (a) the origin is the typical point of the PLCP and (b) the origin is the typical intersection of the PLP.

A. From the typical point

Let the number of intersections from the origin within a distance t be N_t . Furthermore, let $[N_t]$ denote the set $\{1, 2, \dots, N_t\}$. As per the property of PLP, N_t is Poisson distributed with intensity $2\lambda t$ [4]. Accordingly, the complementary cumulative distribution function (CCDF) of D is evaluated as one minus the void probability, which is calculated as follows.

Theorem 1. *Restricted to the single turn case, the distribution of the shortest path length from the typical point of the PLCP to another point of the PLCP is*

$$F_D(t) = 1 - \exp\left(-2\mu t - 2\lambda t + \frac{\lambda}{\mu}(1 - \exp(-2\mu t))\right). \quad (1)$$

Proof: The shortest path length distribution follows directly from the void probability $\mathbb{P}(D > t)$. Let us consider the counting measure notation for the point processes [15], where $\Phi(A)$ denotes the number number of points of Φ within a path length A . Furthermore, Φ_x represents the PPP on L_x . Then, the CCDF is evaluated as:

$$\begin{aligned} \mathbb{P}(D > t) &= \mathbb{P}(\Phi_x(t) = 0, \cup_{i:s_i \leq t} \Phi_i(t - s_i) = 0) \\ &\stackrel{(a)}{=} \mathbb{P}(\Phi_x(t) = 0) \cdot \mathbb{P}(\cup_{i:s_i \leq t} \Phi_i(t - s_i) = 0) \\ &\stackrel{(b)}{=} \exp(-2\mu t) \left[\sum_{k=0}^{\infty} \frac{\exp(-2\lambda t)(2\lambda t)^k}{k!} \left(\frac{1}{t} \int_0^t \exp(-2\mu(t-s)) ds \right)^k \right] \\ &= \exp\left(-2\mu t - 4\lambda t + \frac{2\lambda}{\mu}(1 - \exp(-2\mu t))\right). \end{aligned}$$

The step (a) follows from the independence of the PPPs defined on the lines of the PLP. The step (b) follows from the Poisson distribution of the number of lines. Finally, one minus the void probability gives the relevant distance distribution. ■

Remark 1. *Note that the expression for the void probability is composed of three different terms: $\exp(-2\mu t)$ that represents the probability that no PLCP points is present within t in L_x ; the term $\exp(-4\lambda t)$ corresponds to the event that no line intersects within a distance t from the typical point; while, considering the fact that for the void event, lines can intersect*

within t as long as they do not contain any points within a distance $t - s_i$, the second term is weighted by the positive quantity $\exp\left(\frac{2\lambda}{\mu}(1 - \exp(-2\mu t))\right)$.

B. From the typical intersection

Next, let us consider the typical intersection O depicted in Fig. 4. Here, unlike the previous case, under Palm conditioning, there exists two lines passing through the typical intersection, denoted by L_x and L_y , respectively. To be precise, we define the conditioned line process \mathcal{P}^o as

$$\mathcal{P}^o \triangleq (\mathcal{P} | L_x, L_y \in \mathcal{P}), \quad (2)$$

where L_x and L_y are two lines with a uniformly distributed angle of intersection. Then, under expectation over \mathcal{P}^o , the intersecting point O becomes the typical intersection. Let the angle between L_x and L_y be denoted by θ . Similar to the case of the typical point, the nearest neighbor distribution $\mathbb{P}(D \leq t)$ here is obtained from the void probability depending on path length t . Let the random variable Z_1 denote the length of the lines of \mathcal{P} wherein no point of Φ should be present for the event $D > t$ to hold. First, we characterize Z_1 for different cases of intersection locations of lines L_1 on L_x and L_y . Then, we average out over all possible such L_1 within t to obtain the final result.

Theorem 2. *The distribution of the distance to the nearest PLCP point from the typical intersection of the PLP is*

$$F_D(t) = 1 - \exp(-4\mu t - 2\lambda(2t - \mathcal{T}_x - \mathcal{T}_y)), \quad (3)$$

where

$$\begin{aligned} \mathcal{T}_x &= \frac{1}{\pi^2} \int_0^\pi \int_0^t \int_0^\pi \exp(-\mu Z(x, \omega_1, \omega)) d\omega_1 dx d\omega, \\ \mathcal{T}_y &= \frac{1}{\pi^2} \int_0^\pi \int_0^t \int_{\theta_{\mathcal{E}_{1,1}}}^{\theta_{\mathcal{E}_{1,2}}} \exp(-\mu Z(x, \omega_1, \omega)) d\omega_1 dx d\omega, \end{aligned}$$

and

$$Z(x, \omega_1, \omega) = \begin{cases} 2t - x \left(\frac{\sin \omega - \sin \omega_1}{\sin(\omega_1 - \omega)} + 1 \right); & \omega_1 \in [0, \theta_{\mathcal{E}_{2,1}}] \cup [\theta_{\mathcal{E}_{2,2}}, \pi] \\ 2(t - x); & \theta_1 \in [\theta_{\mathcal{E}_{1,1}}, \theta_{\mathcal{E}_{1,2}}] \\ 4t - 2x \left(1 + \frac{2 \sin \omega_1}{\sin(\omega_1 - \omega)} \right); & \omega_1 \in [\theta_{\mathcal{E}_{2,1}}, \theta_{\mathcal{E}_{1,1}}] \cup [\theta_{\mathcal{E}_{1,2}}, \theta_{\mathcal{E}_{2,2}}]. \end{cases}$$

The ranges of θ_1 in the above equation are as follows.

$$\begin{aligned} \theta_{\mathcal{E}_{1,1}} &= \arctan\left(\frac{t \sin \omega}{t \cos \omega - x}\right), \\ \theta_{\mathcal{E}_{1,2}} &= \arctan\left(\frac{t \sin \omega}{x + t \cos \omega}\right), \\ \theta_{\mathcal{E}_{2,1}} &= \arccos\left(\frac{\left(\left(\frac{2t-x}{x}\right)^2 + 1\right) \cos \omega + 2\left(\frac{2t-x}{x}\right)}{2\left(\frac{2t-x}{x}\right) \cos \omega + \left(\frac{2t-x}{x}\right)^2 + 1}\right), \\ \theta_{\mathcal{E}_{2,2}} &= \arccos\left(\frac{\left(\left(\frac{2t-x}{x}\right)^2 + 1\right) \cos \omega - 2\left(\frac{2t-x}{x}\right)}{-2\left(\frac{2t-x}{x}\right) \cos \omega + \left(\frac{2t-x}{x}\right)^2 + 1}\right). \end{aligned}$$

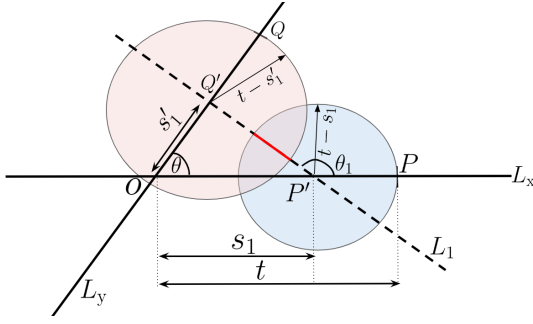


Fig. 4. The single turn case starting from the typical intersection.

Proof: From the typical intersection, under the restriction of at most one turn, we can traverse either L_x or L_y , but not both. Additionally, note that across realizations of \mathcal{P}^o , all the other lines almost surely intersect both L_x and L_y . Let us consider one such line, L_1 , that intersects L_x at P' at a distance s_1 from the origin and L_y at Q' at a distance s'_1 from the origin. Naturally,

$$s'_1 = \frac{s_1 \sin \theta_1}{\sin(\theta_1 - \theta)}. \quad (4)$$

The length of the segment of intersection $|P'Q'|$ has two equivalent forms for given s_1 , θ , and θ_1 :

$$|P'Q'| = \frac{s_1 \sin \theta}{\sin(\theta_1 - \theta)} = \frac{s'_1 \cos \theta - s_1}{\cos \theta_1}, \quad (5)$$

where s'_1 is given by (4). Now conditioned on θ and s_1 consider the following events: (i) the event \mathcal{E}_1^c (complement of event \mathcal{E}_1) defined as the case $s'_1 > t$. In this case, for the shortest path to be of length less than t and the corresponding point to lie on L_1 , the path can only be via the intersection I_{x1} and not via I_{y1} ; and (ii) the joint event $\mathcal{E}_2\mathcal{E}_1$ defined as $|P'Q'| \leq (t - s_1) + (t - s'_1)$ and $s'_1 \leq t$. In this case, the both I_{x1} and I_{y1} are feasible intersection points distances less than t on $P'Q'$. We convert the above conditions on s'_1 to corresponding conditions on θ_1 , given s_1 and θ . Note that $\theta_1 = \arctan\left(\frac{s'_1 \sin \theta}{s'_1 \cos \theta - s_1}\right)$. Thus, for $s'_1 > t$, we have

$$\theta_1 > \arctan\left(\frac{t \sin \theta}{t \cos \theta - s_1}\right) = \theta_{\mathcal{E}_{1,1}}. \quad (6)$$

Similarly, let $\theta_{\mathcal{E}_{1,2}}$ be the angle for which L_1 intersects L_y at a distance t from the origin below the x -axis. For that case, we find a similar angle $\theta_{\mathcal{E}_{1,2}} = \arctan\left(\frac{t \sin \theta}{s_1 + t \cos \theta}\right)$. Thus, the event \mathcal{E}_1^c is equivalent to $\theta_1 \in (\theta_{\mathcal{E}_{1,1}}, \theta_{\mathcal{E}_{1,2}})$. Since for the event \mathcal{E}_1^c , any point within a distance t on L_1 is reachable only from the I_{x1} intersection, for such a point to not exist, we calculate the void probability in a segment of length $Z_1(s_1, \theta, \phi) = 2(t - s_1)$ on L_1 .

Next let us study the event $\mathcal{E}_1\mathcal{E}_2$. Following the same steps as before, we note that if L_1 intersects L_y above the x -axis, then the event \mathcal{E}_2 corresponds to $\frac{s'_1 \sin \theta}{\sin(\theta_1 - \theta)} < 2t - s_1 -$

$\frac{s_1}{\sin(\theta_1 - \theta)}$, or

$$\pi \geq \theta_1 > \arccos\left(\frac{\left(\left(\frac{2t-s_1}{s_1}\right)^2 + 1\right) \cos \theta - 2\left(\frac{2t-s_1}{s_1}\right)}{-2\left(\frac{2t-s_1}{s_1}\right) \cos \theta + \left(\frac{2t-s_1}{s_1}\right)^2 + 1}\right) = \theta_{\mathcal{E}_{2,2}}. \quad (7)$$

On the contrary, in case L_1 intersects L_y below the x -axis, the event \mathcal{E}_2 corresponds to

$$0 \leq \theta_1 \leq \arccos\left(\frac{\left(\left(\frac{2t-s_1}{s_1}\right)^2 + 1\right) \cos \theta + 2\left(\frac{2t-s_1}{s_1}\right)}{2\left(\frac{2t-s_1}{s_1}\right) \cos \theta + \left(\frac{2t-s_1}{s_1}\right)^2 + 1}\right) = \theta_{\mathcal{E}_{2,1}}. \quad (8)$$

Thus, the joint event $\mathcal{E}_1\mathcal{E}_2$ corresponds to $\theta_1 \in [0, \theta_{\mathcal{E}_{2,1}}) \cup (\theta_{\mathcal{E}_{2,2}}, \pi]$. For this case, the length of interest on L_1 where no points should reside is evaluated as

$$Z_1(s_1, \theta, \theta_1) = 2t - s_1 \left(\frac{\sin \theta + \sin \theta_1}{\sin(\theta_1 - \theta)} + 1\right). \quad (9)$$

Finally, for the event $\mathcal{E}_1\mathcal{E}_2^c$, we have $\theta_1 \in [\theta_{\mathcal{E}_{2,1}}, \theta_{\mathcal{E}_{1,1}}) \cup [\theta_{\mathcal{E}_{1,2}}, \theta_{\mathcal{E}_{2,2}}]$. In this case,

$$Z_1(s_1, \theta, \theta_1) = 4t - 2s_1 \left(1 + \frac{\sin \theta_1}{\sin(\theta_1 - \theta)}\right). \quad (10)$$

Let $\mathcal{P}_x \subset \mathcal{P}$ denote the set of lines that intersect L_x within a distance t from the origin. Furthermore, let $\mathcal{P}'_y \subset \mathcal{P}$ denote the set of lines that intersect L_y within a distance t from the origin and intersect L_x outside a distance t from the origin. Based on the above characterization, we proceed with our derivation of the void probability as follows.

$$\begin{aligned} \mathbb{P}(D > t) &= \mathbb{P}(\Phi_x(t) = 0, \Phi_y(t) = 0, \cup_{\mathcal{P}_x} \Phi_i(t - s_i) \\ &\quad \cup_{\mathcal{P}'_y} \Phi_j(t - s'_j) = 0) \\ &= \mathbb{P}(\Phi_x(t) = 0) \mathbb{P}(\Phi_y(t) = 0) \mathbb{P}(\Phi \cap (\cup_{i \in \mathcal{P}_x} Z_i) = 0) \\ &\quad \mathbb{P}(\Phi \cap (\cup_{i \in \mathcal{P}'_y} Z_i) = 0) \\ &= \exp(-4\mu t) \cdot \\ &\quad \left[\sum_{k=0}^{\infty} \frac{p_k(t)}{\pi^2 t} \left(\int_0^\pi \int_0^\pi \int_0^\pi \exp(-\mu Z(x, \omega_1, \omega)) d\omega_1 dx d\omega \right)^k \right] \\ &\quad \left[\sum_{k=0}^{\infty} \frac{p_k(t)}{\pi^2 t} \left(\int_0^\pi \int_0^\pi \int_{\phi_{\mathcal{E}_{1,1}}}^{\phi_{\mathcal{E}_{1,2}}} \exp(-\mu Z(x, \omega_1, \omega)) \right. \right. \\ &\quad \left. \left. d\omega_1 dx d\omega \right)^k \right] \\ &= \exp(-4\mu t - 2\lambda(2t - \mathcal{T}_x - \mathcal{T}_y)). \end{aligned} \quad (11)$$

Remark 2. In Theorem 2, the term $\exp(-4\mu t)$ corresponds to the probability that no point located in either L_x or L_y within a distance t . The term $\exp(-4\lambda t)$ is the probability that no lines should be present with a distance t from the origin along L_x or L_y . However, for the void event such lines can be present given that they do not contain any PLCP points within

a path length t from the origin. Consequently, the probability is augmented by the factor $\exp(2\lambda\mathcal{T}_x) \cdot \exp(2\lambda\mathcal{T}_y)$. The first term takes into account the region along the lines of \mathcal{P}_x while the second term does so for the lines of \mathcal{P}'_y .

Corollary 1 (Zero Turn Case). *The cumulative density function (CDF) of D is lower bound as*

$$F_D(t) \geq 1 - \exp(-4\mu t). \quad (12)$$

Proof: This is derived by considering the void probability of $(\Phi_x \cup \Phi_y) \cap \mathcal{B}(0, t)$, where Φ_x and Φ_y respectively represent the points of Φ on L_x and L_y , and $\mathcal{B}(0, t)$ represents a ball of radius t centered at the typical intersection. ■

Corollary 2 (Upper bound). *The CDF of D is upper bounds as*

$$F_D(t) \leq 1 - \exp(-4(\mu + 4\lambda)t). \quad (13)$$

Proof: The upper bound is derived by considering the void probability of $(\Phi_x \cup \Phi_y \cup \Phi_{I_x} \cup \Phi_{I_y}) \cap \mathcal{B}(0, t)$, where $\cup \Phi_{I_x}$ and $\cup \Phi_{I_y}$ are the intersection in Φ_I present along L_x and L_y , respectively. ■

The above completes an exact characterization of the distribution of the distance to the nearest PLCP point from either the typical point or from the typical intersection restricted to one turn. The next section extends these results to approximate the two-turns case.

IV. TWO TURNS FROM THE TYPICAL POINT

For the two turns case, we restrict our analysis to the case where starting from the origin, we are allowed to move only in a given direction (without loss of generality, let us consider this to be along the positive direction of the x-axis).

Theorem 3. *The distribution of the nearest PLCP point from the typical point of the PLCP under the restriction of two-turns along a single direction is bounded as*

$$\mathbb{P}(D \leq t) \leq 1 - \exp\left(-\lambda \int_0^t 2 - \exp\left(-\lambda \int_0^u 2 - T(w, u) f_{s_i|s_1}(w) dw\right) f_{s_1}(u) du\right), \quad (14)$$

where, $f_{s_i|s_1}(w) = \frac{1}{s_1}$ for $0 \leq w \leq s_1$, $f_{s_1}(u) = \frac{1}{t}$ for $0 \leq u \leq t$. The innermost integrand is

$$T(w, u) = \mathbf{1}(\mathcal{E}_i) \iint_{\theta_i, \theta_1 \in \mathcal{E}_i} \exp(-\mu(t - \left(\frac{u-w}{\cos \theta_i - \sin \theta_i \cot \theta_1} + w\right))) d\theta_1 d\theta_i + (1 - \mathbf{1}(\mathcal{E}_i)) \infty. \quad (15)$$

The event \mathcal{E}_i is defined with the following conditions on θ_i and θ_1 as follows.

$$\mathcal{E}_i = \begin{cases} \theta_1 \leq \cot^{-1}\left(\cos \theta_i - \left(\frac{u-w}{t-w}\right) \csc \theta_i\right); & 0 \leq \theta_i \leq \frac{\pi}{2}, \\ \theta_1 > \cot^{-1}\left(\left(\frac{u-w}{t-w} - \cos \theta_i\right) \csc \theta_i\right); & \frac{\pi}{2} < \theta_i \leq \pi. \end{cases}$$

Proof: Let us consider the intersection formed by two lines L_1 and L_i that cross L_x at distances s_1 and s_i , respectively, from the origin such that $0 \leq s_i \leq s_1 \leq t$. Let us

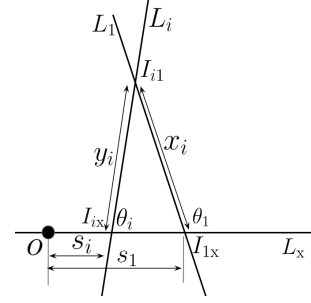


Fig. 5. The two turns case. L_1, L_2, \dots intersect the line L_x .

denote by x_i the distance between the intersection I_{i1} and I_{1X} . Similarly, y_i denotes the distance between I_{i1} and I_{iX} . Naturally, we have

$$x_i = \frac{y_i \sin \theta_i}{\sin \theta_1}, \quad \text{and} \quad y_i = \frac{d_i}{\cos \theta_i - \sin \theta_i \cot \theta_1}.$$

From the intersection I_{i1} , along the line L_1 , we have a remaining path-length budget of $z_i = \max\{0, t - (y_i + s_i)\}$. Thus, we need conditions on θ_1 and θ_i that correspond to the event $\mathcal{E}_i := \{y_i + s_i \leq t\}$. This evaluates to

$$\mathcal{E}_i := \begin{cases} \theta_1 \leq \cot^{-1}\left(\cos \theta_i - \left(\frac{d_i}{t-s_i}\right) \csc \theta_i\right); & 0 \leq \theta_i \leq \frac{\pi}{2}, \\ \theta_1 > \cot^{-1}\left(\left(\frac{d_i}{t-s_i} - \cos \theta_i\right) \csc \theta_i\right); & \frac{\pi}{2} < \theta_i \leq \pi. \end{cases}$$

Accordingly, z_i takes a value 0 in the event \mathcal{E}_i^c (the event that no path length budget remains once we reach I_{i1}) and a value $t - (y_i + s_i)$ in the event \mathcal{E}_i . Let us denote by D_i to be the conditional path length D given that it resides in the line L_1 and is reached via the intersections I_{iX} and I_{i1} . Leveraging the fact that $\Phi \cap [O, I_{iX}]$ and $\Phi \cap [I_{iX}, I_{i1}]$ are independent, we have

$$\begin{aligned} T(s_i, s_1) &= \mathbb{P}(D_i \geq t | s_i, s_1) = \mathbb{P}(\Phi_i((t - (y_i + s_i))^+) = 0) \\ &= \int_0^\pi \int_0^\pi \exp(-\mu z_i) d\theta_1 d\theta_i \\ &= \iint_{\theta_i, \theta_1 \in \mathcal{E}_i} \exp(-\mu(t - (y_i + s_i))) d\theta_1 d\theta_i. \end{aligned}$$

Next, we take into account all s_i such that $0 \leq s_i \leq s_1$. Thanks to the property of the PLP, the number n_1 of such lines is Poisson distributed with parameter $2s_1\lambda$. Accordingly,

$$\begin{aligned} T(s_1) &= \mathbb{P}(\cup_{i: s_i \leq s_1} \Phi_i((t - (y_i + s_i))^+) = 0) \\ &= \mathbb{E}_{n_1, \{s_i\}} [\cup_i T(s_i, s_1)] \\ &\geq \mathbb{E}_{n_1} \left[\prod_{i=1}^{n_1} \mathbb{E}_{s_1} [T(s_i, s_1)] \right] \\ &= \sum_{k=0}^{\infty} \left(\int_0^{s_1} T(w, s_1) f_{s_i|s_1}(w) dw \right)^k \frac{\exp(-2\lambda s_1) (\lambda s_1)^k}{k!} \\ &= \exp\left(-\lambda \int_0^{s_1} 2 - T(w, s_1) f_{s_i|s_1}(w) dw\right), \end{aligned}$$

where $f_{s_i|s_1}(w) = \frac{1}{s_1}$ for $0 \leq w \leq s_1$. Finally, we note that the selected line L_1 could be any of the Poisson number of lines between 0 and t . This implies that the void probability

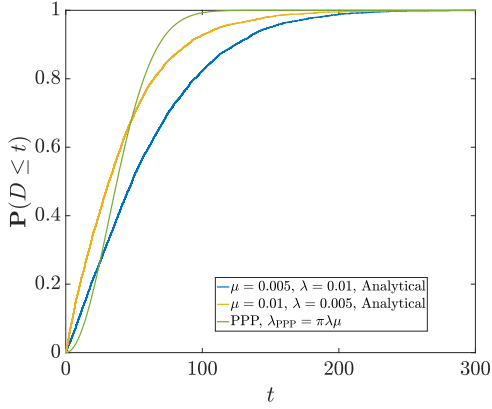


Fig. 6. Single turn case from the typical point and the typical intersection.

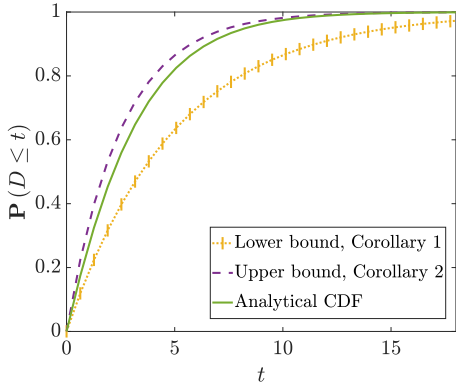


Fig. 7. Single turn case from a typical intersection along with the upper and lower bounds.

is upper bounded by

$$\mathbb{P}(D > t) \geq \exp\left(-\lambda \int_0^t 2 - \exp\left(-\lambda \int_0^u 2 - T(w, u) f_{s_i|s_1}(w) dw\right) f_{s_1}(u) du\right) \quad (16)$$

Finally, the distribution of D follows from the void probability. ■

V. NUMERICAL RESULTS ON THE TRENDS OF THE SHORTEST PATH-LENGTH DISTRIBUTION

Here we discuss the accuracy of the analytical results and the approximation derived for the two turn case. All the quantities are presented as unit less since the model is scale invariant.

Fig. 6 shows that the distance to the nearest PLCP point is statistically closer from the nearest intersection as compared to the nearest point due to the two possible initial paths L_x and L_y available from the typical intersection as compared to only one path available from the typical point. Furthermore, for comparison, we plot the nearest neighbor distribution for a 2D PPP with intensity $\lambda_{PPP} = \mu\lambda$. Interestingly, we see that the CDF is lower for the 2D PPP for lower values of t , while the contrary is true for higher values of t . Indeed, due to the fact that a line passes through the typical point of a PLCP, the nearest point can likely be present on such a line. Based on the values of μ and λ , this may be closer or farther than

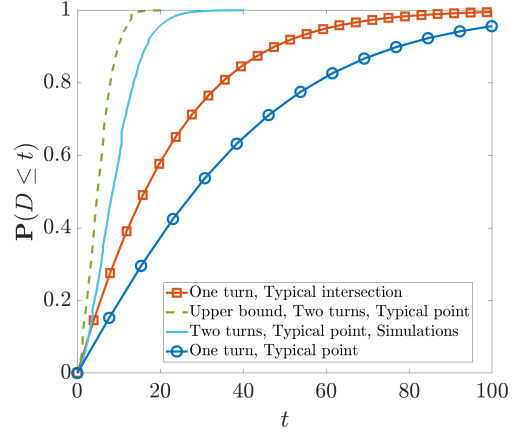


Fig. 8. Comparison of the single turn and turn cases from the typical point and the single turn case from a typical intersection

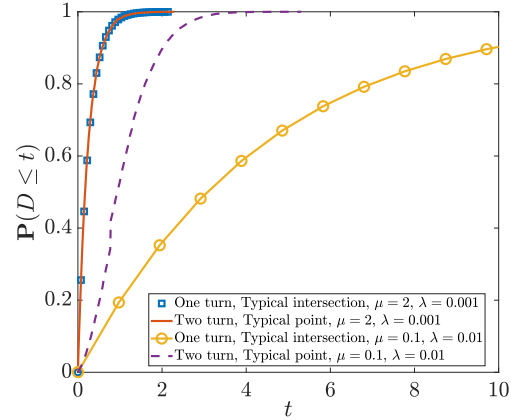


Fig. 9. Comparison of the single turn case from the typical intersection with the two turn case from a typical point for different line and point densities.

the nearest neighbor of a 2D PPP with intensity $\mu\lambda$. However, in case the shortest path to a point is present in a different line than the one passing through the typical PLCP point, its Euclidean distance is smaller than the path length.

Fig. 7 demonstrates the upper and the lower bounds for the shortest path length distribution from the typical intersection as compared to the actual value. Recall that the lower bound is obtained by evaluating the void probability of $(\Phi_x \cup \Phi_y) \cap \mathcal{B}(0, t)$, where Φ_x and Φ_y respectively represent the points of Φ on L_x and L_y . On the contrary, the upper bound follows from the void probability of $(\Phi_x \cup \Phi_y \cup \Phi_{I_x} \cup \Phi_{I_y}) \cap \mathcal{B}(0, t)$, where $\cup \Phi_{I_x}$ and $\cup \Phi_{I_y}$ are the intersection in Φ_I present along L_x and L_y , respectively. Naturally, the lower bound is tighter when μ is higher while the upper bound is tighter when λ is higher. Both the bounds can act as surrogate measures for analysing the performance of wireless networks with low computational complexity. This is discussed further in the next section.

Fig. 8 compares the shortest path length distribution from the typical point and the typical intersection for the single turn case with the same from the typical point for the two turn case. For illustration we have also plotted the analytical bound derived in Theorem 3. Naturally, allowing for two turns statistically brings the nearest point of the PLCP closer. However, Fig. 9 shows that based on the line and point

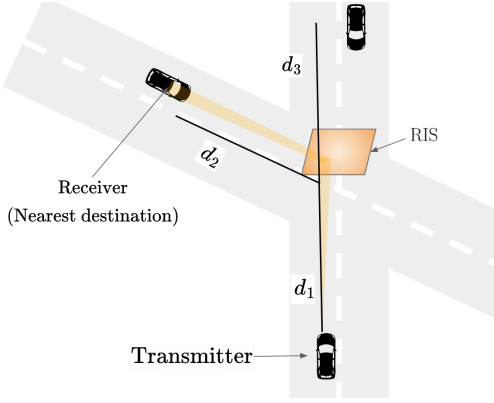


Fig. 10. Illustration of V2V communication using ORIS. The transmitter intends to communicate to the vehicle that will experience the strongest received power. This may be a vehicle present in an intersecting street. Due to the specular reflector model, the received power is a function of the path lengths.

densities, the distance to the nearest point may be same for the two turn case from the typical point and the one turn case from the typical intersection. Indeed, while the former has the benefit of having two starting paths, i.e., along L_x and L_y , the later has the advantage of taking two turns, thereby resulting in the same statistics of the shortest path length, especially for high values of μ and low values of λ . On the contrary, for high λ and/or low μ , the nearest point is much closer to the typical point if two turns are allowed as compared to the typical intersection in case only a single turn is allowed.

VI. APPLICATIONS

A. Near-Field Broadcasting of Basic Safety Messages Leveraging RIS

In RF communications, based on electromagnetic principles, the total gain of the cascaded channel (transmitter-RIS-receiver) is approximately the product of the gains from these two sub-channels and the reflection coefficient of the RIS element, characterizing it as a *multiplicative* channel. In contrast, the channel reflected by an optical re-configurable intelligent surface (ORIS), especially in the near-field and very near-field regime, behaves as an *additive* channel [16], [17]. This behavior is also observed in the near-field broadcasting configuration of RISs even for RF communications [18]. In such near-field transmission, the reflected signal can thus be considered as emanating directly from a virtual transmitter, which is symmetrically positioned relative to the actual transmitter across the plane of the RIS reflecting element.

Accordingly, consider the V2V communication system shown in Fig. 10 where the vehicles intend to transmit basic safety messages (BSMs) to neighboring vehicles as they approach street intersections. The vehicles employ a network-configured PC5 side-link to communicate [19]. Assume that RISs are deployed on the street intersections so that the vehicle on intersecting streets can communicate with each other. Considering the size of the RIS to be large as compared to the transmitting distance, the transmitter can be assumed to be in the near-field of the RIS. For the transmitter, the nearest vehicle (in terms of the path length) may either be on the

same street at a distance $d_1 + d_3$ from the transmitter (as illustrated in the figure), or in the intersecting street at a path length $d_1 + d_2$, connected via the RIS. In case the transmitter leverages the RIS to communicate with the receiver located on the intersecting street, the received signal power in the near-field broadcasting regime is approximated as [18]

$$P_{ri} \approx \frac{G_t G_r \lambda^2 A^2}{16\pi^2 (d_1 + d_i)^2} P_t; \quad i \in \{2, 3\}, \quad (17)$$

where G_t , G_r , and P_t are respectively the transmitter gain, receiver gain, and the transmit power. The carrier wavelength is λ and A is the area of the RIS board. Based on the distances of other vehicles, the nearest receiver corresponds to either $i \in \{2, 3\}$. Let us assume that the receiver is able to decode the BSM packets if the received signal to noise ratio (SNR) is higher than a threshold γ . Naturally, for a noise power N_0 , the probability that the nearest vehicle to the transmitter successfully decodes the BSM packet is evaluated as

$$\begin{aligned} \mathbb{P} \left(\max_i \{P_r\} \geq \gamma \right) &\approx \mathbb{P} \left(\min_i \{d_1 + d_i\} \leq \left(\frac{16\pi^2 \gamma N_0}{G_t G_r \lambda^2 A^2} \right)^{\frac{1}{2}} \right) \\ &= F_D \left(\left(\frac{16\pi^2 \gamma N_0}{G_t G_r \lambda^2 A^2} \right)^{\frac{1}{2}} \right), \end{aligned} \quad (18)$$

which is evaluated using (1).

B. Bound for Far-Field Communications

The shortest path distribution can be used to derive bound on the far-field communication. In particular, the maximum far-field received power with optimized phase responses and no misalignment is given by [18]

$$P_F = \frac{G_t G_r G M^2 N^2 d_x d_y \lambda^2 A^2}{64\pi^3 d_1^2 d_2^2} P_t, \quad (19)$$

where d_x and d_y represent the size of a unit cell along the two dimensions of a square RIS. M and N are respectively the number of RIS elements along the two dimensions. Consequently,

$$\begin{aligned} \mathbb{P}(P_F \geq \gamma) &= \mathbb{P} \left(\frac{G_t G_r G M^2 N^2 d_x d_y \lambda^2 A^2}{64\pi^3 d_1^2 d_2^2} P_t \geq \gamma \right) \\ &= \mathbb{P} \left(d_1 d_2 \leq \sqrt{\frac{64\pi^3}{G_t G_r G M^2 N^2 d_x d_y \lambda^2 A^2}} \right) \\ &\stackrel{(a)}{\geq} \mathbb{P} \left(d_1 + d_2 \leq 2 \left(\frac{64\pi^3}{G_t G_r G M^2 N^2 d_x d_y \lambda^2 A^2} \right)^{\frac{1}{4}} \right) \\ &= F_D \left(2 \left(\frac{64\pi^3}{G_t G_r G M^2 N^2 d_x d_y \lambda^2 A^2} \right)^{\frac{1}{4}} \right), \end{aligned}$$

where the step (a) is from the inequality that the arithmetic mean of d_1 and d_2 is greater than the corresponding geometric mean.

C. Transport Infrastructure Modeling

One of the key bottlenecks for the proliferation of electric vehicles is battery capacity, leading to the requirement of

high density of deployment of charging points across the streets of a city. Researchers have recently employed tools from stochastic geometry to plan for placement of charging points in a city, e.g., see [20]. However, an accurate study of charging point accessibility needs the characterization of the path-lengths. In this regard, the location of such charging points can be modeled as points of a PLCP, while a typical vehicle can be modeled as the typical point of the PLCP. This framework presents several opportunities for mathematical analysis. For example, the shortest path length distributions characterized in this paper can be leveraged to calculate the distance that the typical vehicle needs to travel in order to find the nearest charging point of a given density of streets and the density of charging points. Similarly, as explained in [20], for urban electric bus networks connected via power lines laid throughout the streets, a disconnected bus can get connected to the grid based on the shortest path lengths between busses. Although the authors in [20] did not explore this analytically, possibly due to the lack of an accurate characterization of path length distributions, the results of this paper may aid in such analysis. Furthermore, expanding on the findings, one can analytically describe distance-based cost metrics relevant to transportation systems, such as minimizing travel time and fuel consumption. These insights could be valuable in assessing the response times of medical or police teams arriving at emergency locations and for budgeting of bus and tram stops in a city.

VII. CONCLUSION AND OPEN QUESTIONS

We have derived the shortest path length distribution to a PLCP point from the typical point of a PLCP and the typical intersection of a PLP under the restriction of one turn. Furthermore, we have derived a bound for the shortest path length distribution to a PLCP point from the typical point of a PLCP under the restriction of two turns. Interestingly, for dense point densities and low line densities, the nearest point is closer to the typical intersection restricted to one turn as compared to the same from the typical point restricted to two turns. We highlighted two applications, one on V2V communications using optical links and the other on deployment of electric vehicle charging points, where our derived framework may be employed for statistical analysis.

We are currently investigating the general case, i.e., without a restriction on the number of turns for the shortest path length. Furthermore, percolation questions are open, e.g., what is the probability that there exists an infinitely connected component in terms of the path lengths.

REFERENCES

- [1] B. Ripley, "The foundations of stochastic geometry," *The Annals of Probability*, vol. 4, no. 6, pp. 995–998, 1976.
- [2] F. Baccelli *et al.*, "Stochastic geometry and architecture of communication networks," *Telecommunication Systems*, vol. 7, no. 1, pp. 209–227, 1997.
- [3] C.-S. Choi and F. Baccelli, "Poisson Cox point processes for vehicular networks," *IEEE Transactions on Vehicular Technology*, vol. 67, no. 10, pp. 10 160–10 165, 2018.
- [4] H. S. Dhillon and V. V. Chetlur, "Poisson line Cox process: Foundations and applications to vehicular networks," *Synthesis Lectures on Learning, Networks, and Algorithms*, vol. 1, no. 1, pp. 1–149, 2020.

- [5] J. P. Jeyaraj and M. Haenggi, "Cox models for vehicular networks: SIR performance and equivalence," *IEEE Transactions on Wireless Communications*, vol. 20, no. 1, pp. 171–185, 2020.
- [6] J. P. Jeyaraj *et al.*, "The transdimensional Poisson process for vehicular network analysis," *IEEE Transactions on Wireless Communications*, vol. 20, no. 12, pp. 8023–8038, 2021.
- [7] G. Ghatak, "Binomial line processes: Distance distributions," *IEEE Transactions on Vehicular Technology*, vol. 71, no. 2, pp. 2176–2180, 2021.
- [8] G. Ghatak *et al.*, "Small cell deployment along roads: Coverage analysis and slice-aware RAT selection," *IEEE Transactions on Communications*, vol. 67, no. 8, pp. 5875–5891, 2019.
- [9] F. Morlot, "A population model based on a Poisson line tessellation," in *2012 10th International Symposium on Modeling and Optimization in Mobile, Ad Hoc and Wireless Networks (WiOpt)*, 2012, pp. 337–342.
- [10] V. V. Chetlur, H. S. Dhillon, and C. P. Dettmann, "Shortest path distance in Manhattan Poisson line Cox process," *Journal of Statistical Physics*, vol. 181, pp. 2109–2130, 2020.
- [11] D. M. Nguyen, M. A. Kishk, and M.-S. Alouini, "Modeling and analysis of dynamic charging for EVs: A stochastic geometry approach," *IEEE Open Journal of Vehicular Technology*, vol. 2, pp. 17–44, 2020.
- [12] C. Gloaguen *et al.*, "Analysis of shortest paths and subscriber line lengths in telecommunication access networks," *Networks and Spatial Economics*, vol. 10, no. 1, pp. 15–47, 2010.
- [13] N. Miyoshi, "Neveu's exchange formula for analysis of wireless networks with hotspot clusters," *Frontiers in Communications and Networks*, vol. 3, p. 885749, 2022.
- [14] F. Voss, C. Gloaguen, and V. Schmidt, "Scaling limits for shortest path lengths along the edges of stationary tessellations," *Advances in Applied Probability*, vol. 42, no. 4, pp. 936–952, 2010.
- [15] S. N. Chiu, D. Stoyan, W. S. Kendall, and J. Mecke, *Stochastic geometry and its applications*. John Wiley & Sons, 2013.
- [16] S. Sun *et al.*, "Optical intelligent reflecting surface assisted MIMO VLC: Channel modeling and capacity characterization," *IEEE Transactions on Wireless Communications*, 2023.
- [17] —, "Optical IRS for Visible Light Communication: Modeling, Design, and Open Issues," *arXiv preprint arXiv:2405.18844*, 2024.
- [18] W. Tang, M. Z. Chen, X. Chen, J. Y. Dai, Y. Han, M. Di Renzo, Y. Zeng, S. Jin, Q. Cheng, and T. J. Cui, "Wireless communications with reconfigurable intelligent surface: Path loss modeling and experimental measurement," *IEEE transactions on wireless communications*, vol. 20, no. 1, pp. 421–439, 2020.
- [19] R. Molina-Masegosa, J. Gozalvez, and M. Sepulcre, "Configuration of the C-V2X mode 4 sidelink PCS interface for vehicular communication," in *2018 14th International conference on mobile ad-hoc and sensor networks (MSN)*. IEEE, 2018, pp. 43–48.
- [20] R. Atat, M. Ismail, and E. Serpedin, "Stochastic geometry planning of electric vehicles charging stations," in *ICASSP 2020-2020 IEEE International Conference on Acoustics, Speech and Signal Processing (ICASSP)*. IEEE, 2020, pp. 3062–3066.